

# Pain-related behaviors and neurochemical alterations in mice expressing sickle hemoglobin: modulation by cannabinoids

\*Divyanshoo R. Kohli,<sup>1</sup> \*Yunfang Li,<sup>1</sup> Sergey G. Khasabov,<sup>2</sup> Pankaj Gupta,<sup>3</sup> Lois J. Kehl,<sup>4</sup> Marna E. Ericson,<sup>5</sup> Julia Nguyen,<sup>1</sup> Vinita Gupta,<sup>6</sup> Robert P. Hebbel,<sup>1</sup> Donald A. Simone,<sup>2</sup> and Kalpna Gupta<sup>1</sup>

<sup>1</sup>Vascular Biology Center, Division of Hematology, Oncology & Transplantation, Department of Medicine, and <sup>2</sup>Department of Diagnostic & Biological Sciences, University of Minnesota, Minneapolis; <sup>3</sup>Division of Hematology, Oncology & Transplantation, Department of Medicine, University of Minnesota and Veterans Administration Medical Center, Minneapolis; <sup>4</sup>Minnesota Head and Neck Pain Clinic, St Paul; <sup>5</sup>Department of Dermatology, University of Minnesota, Minneapolis; and <sup>6</sup>Bio-Rad Laboratories, Hercules, CA

**Sickle cell disease causes severe pain. We examined pain-related behaviors, correlative neurochemical changes, and analgesic effects of morphine and cannabinoids in transgenic mice expressing human sickle hemoglobin (HbS). Paw withdrawal threshold and withdrawal latency (to mechanical and thermal stimuli, respectively) and grip force were lower in homozygous and hemizygous Berkley mice (BERK and hBERK1, respectively) compared with control mice expressing human hemoglobin A (HbA-BERK), indicating deep/musculoskeletal and cutaneous hyperalgesia. Peripheral nerves and blood vessels were structurally altered in BERK and hBERK1 skin, with decreased expression of  $\mu$  opioid receptor and increased calcitonin gene-related peptide and substance P immunoreactivity. Activators of neuropathic and inflammatory pain (p38 mitogen-activated protein kinase, STAT3, and mitogen-activated protein kinase/extracellular signal-regulated kinase) showed increased phosphorylation, with accompanying increase in COX-2, interleukin-6, and Toll-like receptor 4 in the spinal cord of hBERK1 com-**

**pared with HbA-BERK. These neurochemical changes in the periphery and spinal cord may contribute to hyperalgesia in mice expressing HbS. In BERK and hBERK1, hyperalgesia was markedly attenuated by morphine and cannabinoid receptor agonist CP 55940. We show that mice expressing HbS exhibit characteristics of pain observed in sickle cell disease patients, and neurochemical changes suggestive of nociceptor and glial activation. Importantly, cannabinoids attenuate pain in mice expressing HbS. (*Blood*. 2010;116(3):456-465)**

**pared with HbA-BERK. These neurochemical changes in the periphery and spinal cord may contribute to hyperalgesia in mice expressing HbS. In BERK and hBERK1, hyperalgesia was markedly attenuated by morphine and cannabinoid receptor agonist CP 55940. We show that mice expressing HbS exhibit characteristics of pain observed in sickle cell disease patients, and neurochemical changes suggestive of nociceptor and glial activation. Importantly, cannabinoids attenuate pain in mice expressing HbS. (*Blood*. 2010;116(3):456-465)**

## Introduction

Sickle cell disease (SCD) is accompanied by acute painful episodes (“crises”) superimposed on chronic pain.<sup>1</sup> Pain in SCD starts early in life, increases in severity with age, and is particularly difficult to treat. The pathophysiology of SCD is compounded by inflammation, vasculopathy, ischemia-reperfusion injury, organ damage, and neuropathy, each of which may contribute to pain. For example, behaviorally, “crises” result in acute episodes of severe pain, whereas ensuing tissue and/or bone damage leads to persistent pain. In addition, inflammation in SCD may potentiate both episodic and persistent pain. Clinical studies show marked variability in pain presentation, resulting from diverse factors, including geographic location, sex, age, and temperature, demonstrating the complexity of pain in SCD.<sup>1-3</sup> The mechanisms underlying chronic pain in SCD remain poorly defined.

Opioids are the mainstay of treatment for severe pain associated with SCD.<sup>3</sup> High doses of opioids are required because of altered pharmacokinetics of morphine and increased clearance.<sup>4-6</sup> The efficacy of long-term opioid administration is also impaired by the development of opioid tolerance or opioid-induced hyperalgesia (see Table 1 for definitions). Further, chronic opioid use in SCD may lead to adverse effects on peripheral systems, including renal toxicity and acute chest syndrome.<sup>7,8</sup> Identification of alternative or adjunctive analgesic agents is therefore needed.

Cannabinoids offer a novel approach to treat chronic pain and hyperalgesia.<sup>9-13</sup> Inhaled or systemically injected cannabinoids are effective in treating pain in HIV/AIDS and multiple sclerosis and breakthrough pain in cancer.<sup>9,13,14</sup> Activation of peripheral cannabinoid receptors attenuates hyperalgesia in inflammation and cancer.<sup>9</sup> Selective pharmacologic activation of peripheral cannabinoid receptors to attenuate pain is particularly appealing because it might avoid side effects associated with activation of cannabinoid receptors in the central nervous system. Because pain in SCD may have both inflammatory and neuropathic components, we hypothesized that cannabinoids may provide pain relief in SCD.

Both inflammatory and nociceptive stimuli activate the mitogen-activated protein kinase (MAPK) family of kinases, including p38 and extracellular signal-regulated kinase (ERK) in primary sensory neurons, leading to the sensitization of nociceptors and activation of spinal glial cells,<sup>15</sup> which contributes to facilitation of pain transmission at the level of the spinal cord (central sensitization). Nociceptor sensitization may lead to an increase in release of calcitonin gene-related peptide (CGRP) and substance P (SP) from peripheral nerve endings, causing neurogenic inflammation and hyperalgesia.<sup>16</sup> This vicious cycle of inflammatory and nociceptive insult followed by nociceptor sensitization may thus contribute to increased hyperalgesia and chronic pain. However, it is unknown

Submitted January 14, 2010; accepted March 5, 2010. Prepublished online as *Blood* First Edition paper, March 19, 2010; DOI 10.1182/blood-2010-01-260372.

\*D.R.K. and Y.L. contributed equally to this study.

An Inside *Blood* analysis of this article appears at the front of this issue.

The online version of this article contains a data supplement.

The publication costs of this article were defrayed in part by page charge payment. Therefore, and solely to indicate this fact, this article is hereby marked “advertisement” in accordance with 18 USC section 1734.

© 2010 by The American Society of Hematology

**Table 1. Definitions of pain-related terminology**

Term	Definition
Nociception	The neural processes of encoding and processing noxious stimuli
Nociceptors	A receptor on primary afferent fibers preferentially sensitive to a noxious stimulus or to a stimulus that would become noxious if prolonged
Hyperalgesia	An increase in pain to a stimulus that is normally painful
Allodynia	Pain evoked by a stimulus that does not normally provoke pain
Central sensitization	Enhanced excitability of nociceptive neurons in the dorsal horn of spinal cord resulting from tissue damage or inflammation
Neuropathic pain	Pain initiated or caused by a primary lesion or dysfunction in the nervous system
Nocifensive behavior	Behavioral responses to noxious stimuli

whether these signaling pathways are activated and contribute to pain in SCD.

SCD in humans, and transgenic mice expressing sickle hemoglobin (HbS), share the presence of a systemic inflammatory state.<sup>17,18</sup> One such mouse model exhibits facilitation of the tail flick reflex,<sup>19</sup> suggesting enhanced nociception in this model. In the present studies, we used an array of behavioral measures to characterize pain in transgenic mice expressing human HbS, and assessed the analgesic effects of opioids and cannabinoids. We also investigated morphologic and biochemical changes in primary afferent neurons and in the spinal cord. We show that peripheral vascular insult is paralleled by cutaneous and deep hyperalgesia, and is attenuated by opioids and cannabinoids. Structural and neurochemical changes were identified in the periphery and spinal cord, which may contribute to hyperalgesia in mice expressing HbS.

## Methods

Detailed methods are provided in the supplemental Methods (available on the *Blood* Web site; see the Supplemental Materials link at the top of the online article).

### Mice

We used 2 transgenic murine models that express human HbS and a control mouse that expresses normal human hemoglobin A.

Berkley (BERK) mice are homozygous for knockout of both murine  $\alpha$  and  $\beta$  globins and carry a single copy of the linked transgenes for human  $\alpha$  and  $\beta^S$  globins. Therefore, BERK mice express human  $\alpha$  and  $\beta^S$  globin chains (thus, human hemoglobin S), but no murine  $\alpha$  or  $\beta$  globins.<sup>20</sup> They have severe disease that simulates human sickle cell anemia (hemolysis, reticulocytosis, anemia, extensive organ damage, and shortened life span).<sup>20</sup>

hBERK1 mice are homozygous for knockout of murine  $\alpha$  globin, hemizygous for knockout of murine  $\beta$  globin, and carry a single copy of the linked transgenes for human  $\alpha$  and  $\beta^S$  globins.<sup>20</sup> hBERK mice express the following globin chains: human  $\alpha$ , human  $\beta^S$ , and murine  $\beta$  (thus, human hemoglobin S and a hybrid human  $\alpha$ /mouse  $\beta$  hemoglobin).<sup>21</sup> Both BERK and hBERK1 are on the same mixed genetic background and are bred as littermates.

Control HbA-BERK mice have the same mixed background as BERK and hBERK1 but exclusively express human  $\alpha$  and  $\beta^A$  globins (thus, normal human hemoglobin A) but no murine  $\alpha$  or  $\beta$  globins.<sup>20</sup>

Mice were bred in a pathogen-free facility, maintained under controlled environmental conditions (12 hours light-to-dark cycle, at 23°C), and were genotyped and phenotyped as described by us.<sup>18</sup> Experiments were

approved by the Institutional Animal Care and Use Committee at the University of Minnesota.

### Drugs and their use

**Effect of opioids and cannabinoids on deep hyperalgesia.** HbA-BERK, BERK, and hBERK1 mice were given 10 or 20 mg/kg morphine sulfate intraperitoneally in a volume of 100  $\mu$ L. Grip force was determined before and at 1, 2, 4, and 24 hours after injection. Dose of morphine was selected based on the standard dose of morphine used in mouse models of other chronic painful conditions, which is approximately 10 mg/kg.<sup>22</sup> ED<sub>50</sub> doses of morphine in different strains of mice for analgesia range from approximately 4 to 12 mg/kg, which are much higher relative to morphine dose in humans.<sup>23</sup> This could be the result of shorter half-life of morphine (~42 minutes) in mice compared with humans (2-4 hours).<sup>24</sup>

The cannabinoid receptor agonist, (-)-cis-3-[2-hydroxy-4(1,1-dimethylheptyl)phenyl]-trans-4-(3-hydroxypropyl) cyclohexanol (CP 55940; Tocris Bioscience) was prepared in 5% emulphor, 5% ethanol, and 90% normal saline. Separate groups of HbA-BERK, BERK, and hBERK1 mice received 0.3 mg/kg CP 55940 intraperitoneally in a volume of 0.1 mL/10 g body weight. Grip force and catalepsy (bar test described in the supplemental Methods) were determined before and at 0.5, 1, 1.5, 3, 6, and 24 hours after injection.

### Modulation of inflammatory hyperalgesia by activation of peripheral cannabinoid receptors

Inflammation of the left hind paw was produced in mice by intraplantar injection of 10  $\mu$ g (in 10  $\mu$ L) complete Freund adjuvant (CFA; Sigma-Aldrich). Paw withdrawal frequency (PWF) evoked by the application of the 1.0 g von Frey monofilament was determined before and at 24 hours after CFA. Mice then received an intraplantar injection of the cannabinoid receptor agonist CP 55940 (10  $\mu$ g in 10  $\mu$ L) or vehicle, and PWF and time spent on the bar (bar test) were determined at 1, 3, and 6 hours after injection.

### Pain-related behaviors

**Grip force.** To evaluate deep tissue hyperalgesia, forepaw grip force was measured using a computerized grip force meter.

**Mechanical hyperalgesia.** To assess sensitivity to a mechanical stimulus, paw withdrawal threshold and PWF evoked by calibrated von Frey (Semmes-Weinstein) monofilaments (Stoelting) were determined.

**Heat hyperalgesia.** Paw withdrawal latency (PWL) was recorded in response to a radiant heat stimulus applied to the plantar surface of a single hind paw from underneath a glass floor with a projector lamp bulb.

**Cold hyperalgesia.** The latency to initial lifting of either forepaw on cold plate (4°C) and the number of times mice lifted or rubbed the forepaws together (PWF) over a period of 2 minutes were determined.

### Histology, laser scanning confocal microscopy, and immunofluorescence microscopy

For laser scanning confocal microscopy, sections were immunostained using the following primary antibodies: lymphatic vessels, 1:500 goat anti-LYVE 1 (R&D Systems); blood vessels, 1:200 rat anti-CD31 (Santa Cruz Biotechnology); and peripheral nerves, 1:1000 rabbit anti-PGP 9.5 (Biogenesis), 1:200 anti-CGRP (Abcam), and 1:200 anti-SP (Serotec). This was followed by staining with species specific secondary antibodies labeled with Cy2, Cy3, and Cy5 (Jackson ImmunoResearch). In parallel, control primary antibodies were substituted by isotype-matched IgG. A montage of overlapping fields of view was prepared from the Z-stack images of 1.62  $\mu$ m each, acquired using a FluoView FV1000 Laser Scanning Confocal Microscope (Olympus America).

For immunofluorescence microscopy, cryosections were immunostained with 1:100 anti- $\mu$  opioid receptor (MOR; Chemicon International), 1:50 anti-CD31-PE (BD Biosciences Pharmingen), and 4,6-diamidino-2-phenylindole (Invitrogen), as described by us previously.<sup>25</sup> Isotype-matched primary antibody controls included rabbit anti-mouse IgG and rat anti-mouse IgG (Jackson ImmunoResearch).

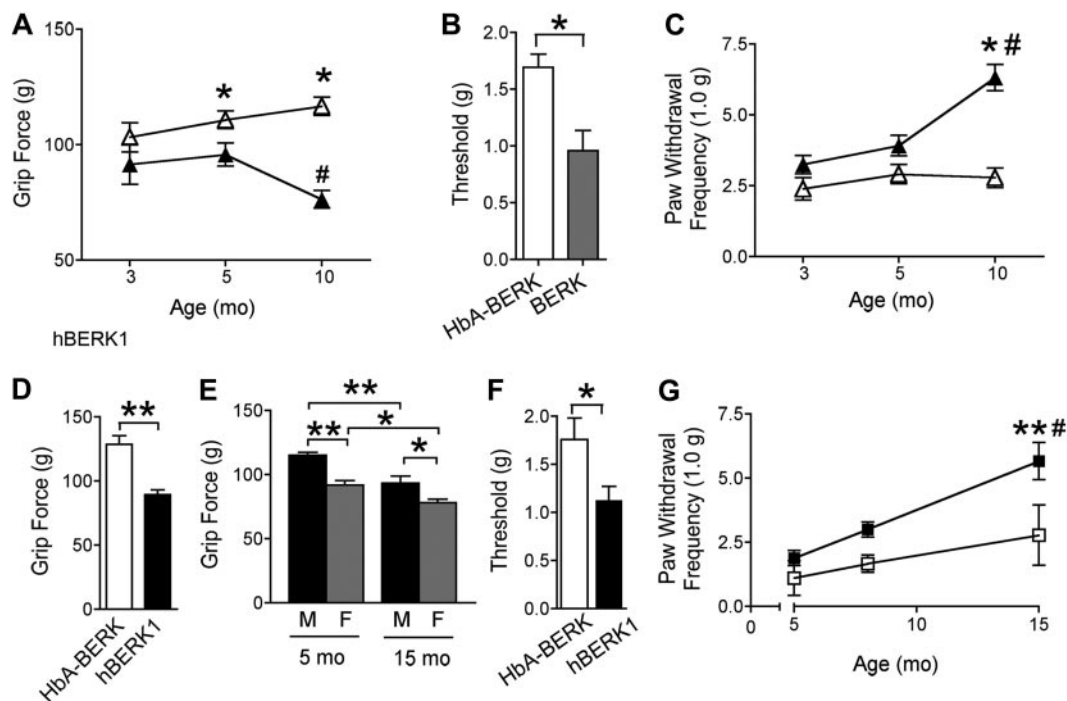


**Figure 1. BERK and hBERK1 mice show deep tissue and mechanical hyperalgesia.** All data are shown as mean  $\pm$  SEM from 4 to 6 mice with 3 observations per mouse. Measurements were made on each mouse on 3 consecutive days. (A) Grip force measurements from age-matched BERK ( $\blacktriangle$ ) and HbA-BERK ( $\triangle$ ) mice. A lower grip force indicates increased deep tissue hyperalgesia.  $*P < .05$  versus age-matched BERK.  $\#P < .01$  versus 3-month-old BERK. (B) Paw withdrawal threshold (50%) to von Frey monofilaments in 10-month-old BERK and HbA-BERK mice.  $*P < .05$ . (C) PWF with a von Frey monofilament in BERK ( $\blacktriangle$ ) and age-matched HbA-BERK ( $\triangle$ ). A higher PWF indicates increased nociception.  $*P < .05$  versus age-matched HbA-BERK.  $\#P < .01$  versus 3-month-old BERK. (D) Grip force measurements from 12-month-old male hBERK1 mice compared with age- and sex-matched HbA-BERK mice. A lower grip force indicates increased deep tissue hyperalgesia.  $**P < .01$ . (E) Effect of age and sex on grip force in hBERK1 mice (M indicates male; F, female).  $*P < .05$ ,  $**P < .01$  between the indicated conditions. (F) Paw withdrawal threshold (50%) using von Frey monofilaments in 9- to 10-month-old female hBERK1 mice compared with age- and sex-matched HbA-BERK mice. A lower threshold is indicative of increased sensitivity to nociceptive stimuli.  $*P < .05$ . (G) PWF with von Frey monofilaments in male hBERK1 mice ( $\blacksquare$ ) compared with HbA-BERK mice ( $\square$ ) at different ages. A higher PWF reflects increased nociception.  $**P < .01$ , significant differences (15-month vs 5-month hBERK1).  $\#P < .01$ , significant differences (15-month hBERK1 vs 15-month HbA-BERK).

### Western immunoblotting of brain and whole spinal cord lysates

Western immunoblotting was performed using antibodies to phospho-p38 MAPK (p38 MAPK-Thr180/Tyr182), total p38, ERK (MAPK/ERK-Thr202/Tyr204), total p44/42 MAPK/ERK; phospho-signal transducer and activator of transcription 3 (STAT3-Tyr705), and total STAT3 (79D7; all from Cell Signaling Technology).

### Reverse-transcribed polymerase chain reaction

RNA from whole spinal cords and brains was analyzed for transcripts of cyclo-oxygenase 2 (COX-2), MOR, interleukin 6 (IL-6), Toll-like receptor 4 (TLR-4), and glyceraldehyde 3-phosphate dehydrogenase (GAPDH). The polymerase chain reaction products were sequenced to verify the expected DNA sequences.

### Statistical analysis

Information on statistical analysis is contained in supplemental Methods.

## Results

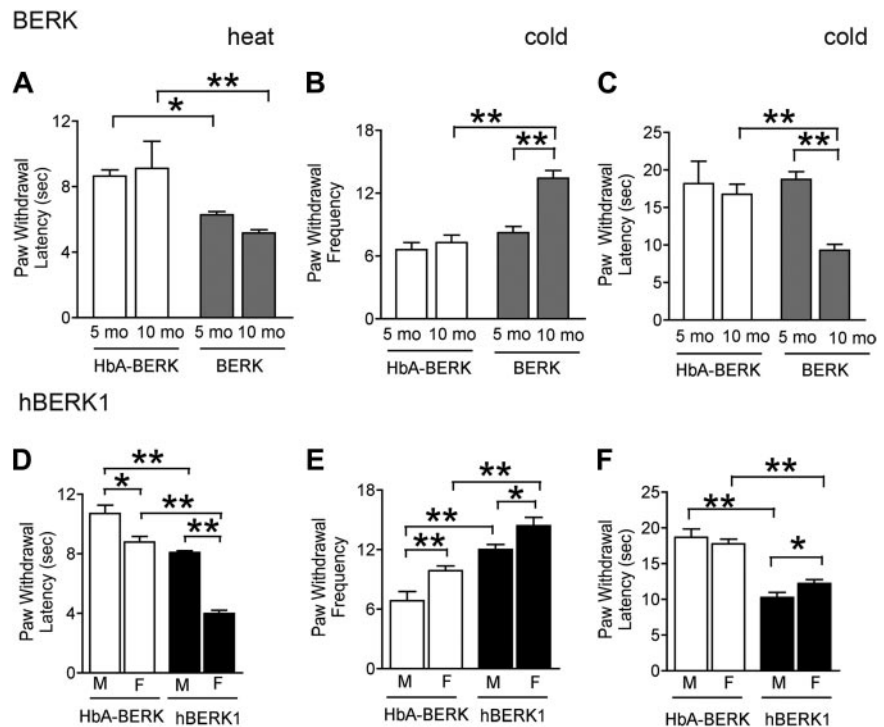
Behavioral, histochemical, and morphologic approaches were used to characterize pain-related behaviors and investigate underlying mechanisms in the periphery and spinal cord. We also observed pathologic changes in the vasculature and in morphology and chemistry of peripheral nerves, as well as changes in glial activation in the spinal cord that may contribute to persistent pain and hyperalgesia.

### Mice expressing HbS exhibit deep and cutaneous hyperalgesia

**Deep hyperalgesia.** Because chronic musculoskeletal pain is a frequent consequence of SCD, we tested for musculoskeletal pain in BERK and hBERK1 mice in the absence of any traumatic/vascular/inflammatory insult, using the grip force test. A lower force indicates increased nociception. Grip force decreased with increasing age in both BERK and hBERK1 mice (Figure 1A,E). BERK and hBERK1 had lower grip force compared with age- and sex-matched control HbA-BERK mice (Figure 1D). hBERK1 females showed significantly lower grip force compared with age-matched males (Figure 1E). These data indicate the presence of spontaneous, chronic deep tissue/musculoskeletal hyperalgesia in hBERK1 and BERK mice, which increases with age.

**Mechanical hyperalgesia.** Paw withdrawal thresholds determined using von Frey monofilaments were lower in mice expressing HbS. Withdrawal threshold in 10- and 8-month-old BERK and hBERK1, respectively, were lower than in HbA-BERK mice (Figure 1B,F). Similarly, PWF evoked by the standard monofilament (1.0 g; 4.08 mN) was higher in mice expressing HbS compared with HbA-BERK (Figure 1C,G). HbA-BERK mice did not show any significant age-related changes in PWF (Figure 1C,G). PWF increased consistently with age in both BERK and hBERK1 (Figure 1C,G). Thus, paw withdrawal threshold is decreased and PWF is increased in both BERK and hBERK1, suggesting that these mice have mechanical hyperalgesia, which increases further with age.

**Figure 2. BERK and hBERK1 mice show increased heat and cold hyperalgesia.** PWL after application of a heat stimulus (A,D) and nocifensive behaviors on a cold plate at  $4 \pm 1^\circ\text{C}$  (B-C,E-F) were recorded for each mouse. Shorter PWL (in seconds) in response to heat stimulus is indicative of increased thermal hyperalgesia. A higher PWF in a 2-minute period and lower PWL on a cold plate are indicative of increased sensitivity to cold-induced nociception. Data are the mean  $\pm$  SEM from 4 to 6 mice with 3 observations per mouse. Significance of differences between the indicated conditions in each panel: \* $P < .05$ , \*\* $P < .01$ . (A) PWL after a heat stimulus in age- and sex-matched BERK and HbA-BERK mice. (B) PWF on a cold plate in age- and sex-matched BERK and HbA-BERK mice. (C) PWL on a cold plate in age- and sex-matched BERK and HbA-BERK mice. (D) PWL after a heat stimulus in 9-month-old hBERK1 and age-matched HbA-BERK mice. (E-F) PWF (E) and PWL (F) on a cold plate in 15-month-old hBERK1 and age-matched HbA-BERK mice. M indicates male; F, female.



**Heat hyperalgesia.** Decrease in PWL was observed in 5- and 10-month-old male BERK (Figure 2A) as well as in 8-month-old male and female hBERK1 (Figure 2D) mice, compared with age- and sex-matched HbA-BERK controls. Female HbA-BERK and hBERK1 mice had shorter PWL compared with their male counterparts. Because shorter PWL indicates increased sensitivity to heat, these data suggest that BERK and hBERK1 mice have enhanced sensitivity to heat.

**Cold hyperalgesia.** We examined sensitivity to cold in 5- and 10-month-old BERK (Figure 2B-C), 15-month-old hBERK1 (Figure 2E-F), and age- and sex-matched HbA-BERK mice using a cold plate maintained at  $4^\circ\text{C}$ . Older (10 months) but not younger (5 months) BERK exhibited higher PWF and shorter PWL compared with age-matched HbA-BERK mice. Fifteen-month-old hBERK1 of both sexes exhibited increased sensitivity to cold compared with age- and sex-matched HbA-BERK mice. Female hBERK1 had a higher PWF and shorter PWL compared with males. No significant differences were seen between female and male BERK mice (data not shown). Female HbA-BERK controls showed higher PWF compared with males, but no difference in PWL. Thus, sensitivity to cold was greater in BERK and hBERK1 compared with HbA-BERK mice.

#### Effect of morphine and cannabinoid receptor agonist CP 55940 on deep tissue hyperalgesia

Because morphine is used to treat pain in patients with SCD, we examined whether morphine can reduce deep tissue hyperalgesia in BERK and hBERK1 mice (Figure 3A,C). We also examined whether the cannabinoid receptor agonist CP 55940 would attenuate deep hyperalgesia in BERK and hBERK1 mice (Figure 3B,D). Injection of 20 mg/kg, but not 10 mg/kg, morphine increased grip force in BERK (Figure 3A) and hBERK1 (Figure 3C) mice from 1 to 4 hours after treatment. Grip force returned to preinjection levels by 24 hours after injection.

Similar to the effect produced by 20 mg/kg morphine, systemic (intraperitoneal) administration of only 0.3 mg/kg CP 55940 also

increased grip force in both BERK (Figure 3B) and hBERK1 (Figure 3D) mice, from 0.5 to 6 hours after injection compared with pretreatment (baseline) values and compared with vehicle. Grip force returned to baseline values by 24 hours after injection. Morphine and CP 55940 had no effect on grip force in age- and sex-matched control HbA-BERK mice (supplemental Figure 1A-B). CP 55940 did not produce catalepsy (supplemental Figure 1C-D). These data indicate that, as in humans with SCD, morphine attenuates musculoskeletal pain in BERK and hBERK1 mice and further that low doses of cannabinoids may be effective in attenuating deep tissue pain in these mice.

#### Local administration of CP 55940 attenuates CFA-induced pain

Systemic administration of CP 55940 attenuated hyperalgesia without producing catalepsy, suggesting that the antihyperalgesia effect was mediated by peripheral mechanisms. We therefore investigated whether direct activation of peripheral cannabinoid receptors by local intraplantar administration of CP 55940 (10  $\mu\text{g}$  in 10  $\mu\text{L}$ ) would attenuate mechanical hyperalgesia. We evaluated the effects of CP 55940 after localized inflammation induced by CFA (Figure 4) to mimic the localized acute pain and inflammation that occur in SCD. All mice (BERK, hBERK1, and HbA-BERK) exhibited an increase in PWF to the standard von Frey monofilament at 24 hours after intraplantar injection of CFA in the left hind paw. Injection of CP 55940, but not vehicle, reduced the CFA-induced increase in PWF in BERK and hBERK1 mice. CP 55940 did not have any effect on age- and sex-matched HbA-BERK mice (supplemental Figure 1). CP 55940 did not produce catalepsy (supplemental Figure 2), suggesting that the antihyperalgesic effect of CP 55940 was the result of activation of peripheral and not central cannabinoid receptors.

#### Alterations in the architecture of dermal blood vessels, nerves, and lymphatics in BERK and hBERK1 mice

To examine whether changes in the structure of the skin and cutaneous innervation might contribute to increased hyperalgesia,



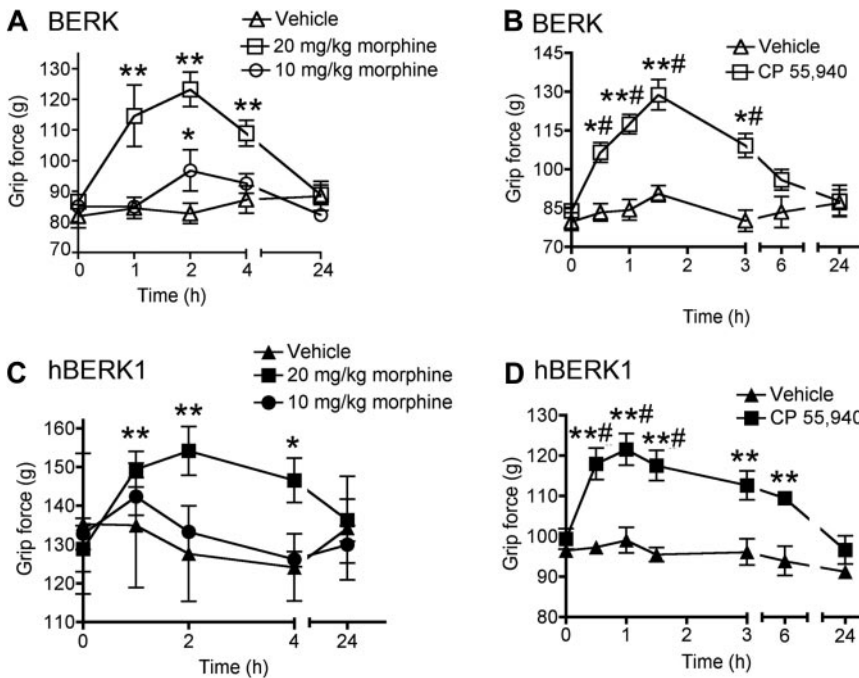


**Figure 3. Morphine and CP 55940 treatment reduce nociceptive behaviors in BERK and hBERK1 mice.** Mice were injected intraperitoneally with morphine or vehicle (A,C) and 0.3 mg/kg CP 55940 or vehicle (B,D), and grip force responses were recorded over the indicated time period. An increase in grip force indicates a decrease in nociception. All data are shown as mean  $\pm$  SEM from 4 to 6 mice with 3 observations per mouse. Significance of differences: In panel A: \* $P < .05$ , \*\* $P < .01$  versus baseline at 0 hours (immediately before treatment). In panel B: \* $P < .05$ , \*\* $P < .01$  versus baseline; # $P < .01$  versus vehicle at the same time point. In panel C: \* $P < .05$ , \*\* $P < .01$  versus baseline. In panel D: # $P < .01$  versus baseline; \*\* $P < .01$  versus vehicle at the same time point.

we examined the skin of BERK and hBERK1 and control HbA-BERK mice. Control HbA-BERK mice (Figure 5A) showed normal vascular architecture replete with plexuses of blood vessel and nerves and well-organized branching of dense nerve fibers and blood vessels in the dermis. Nerve fibers and blood vessels ran parallel to and wrapped around each other. Blood vessels and nerves surrounded the hair follicles. The lymphatic vessels appeared wide, with open ends facing the epidermis. The peripheral nerve fibers ran parallel to blood vessels, and the nerve plexuses ran parallel to the vascular plexuses in the deep dermis.

In contrast, the architecture of nerve plexus and PGP9.5 immunoreactive peripheral nerve fibers was distorted in both BERK and hBERK1 mice. Compared with HbA-BERK, fewer nerve fibers were seen in the dermis and were haphazardly oriented with respect to the blood vessels. hBERK1 mice showed moderately abnormal structure and organization of blood vessels, nerves, and lymphatics (Figure 5B), with loss of the normal association of these structures. Further, in hBERK1 mice, vascular plexuses were absent and blood vessels were markedly

diminished in the deep dermis; the few remaining vessels were disorganized and frequently invaded the epidermis. The lymphatics were stringy and loosely oriented compared with HbA-BERK mice. All these structures were even more abnormal in BERK mice (Figure 5C-D). Higher magnification of BERK skin (Figure 5D) showed collateralization of nerve fibers and sprouting (shown in the inset). These abnormalities were accompanied by significant thinning of the epidermis and dermis in hBERK1 and BERK compared with HbA-BERK mice (Figure 5E; supplemental Figure 3). These data suggest that sickle vasculopathy is accompanied by marked perturbation of peripheral nerve fibers and lymphatics in the skin and reduction in epidermal and dermal thickness.

**Elevation of SP and CGRP, and reduction in MOR expression in mice expressing HbS**

We next investigated whether changes also occurred in neurochemistry. We determined whether the expression of SP and CGRP,

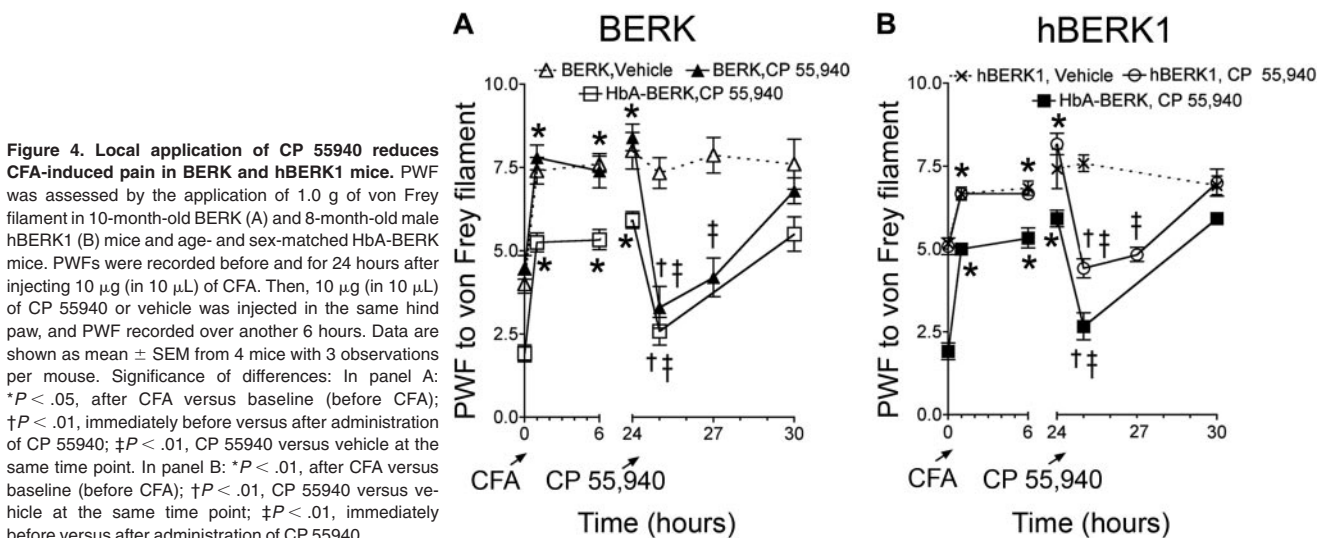
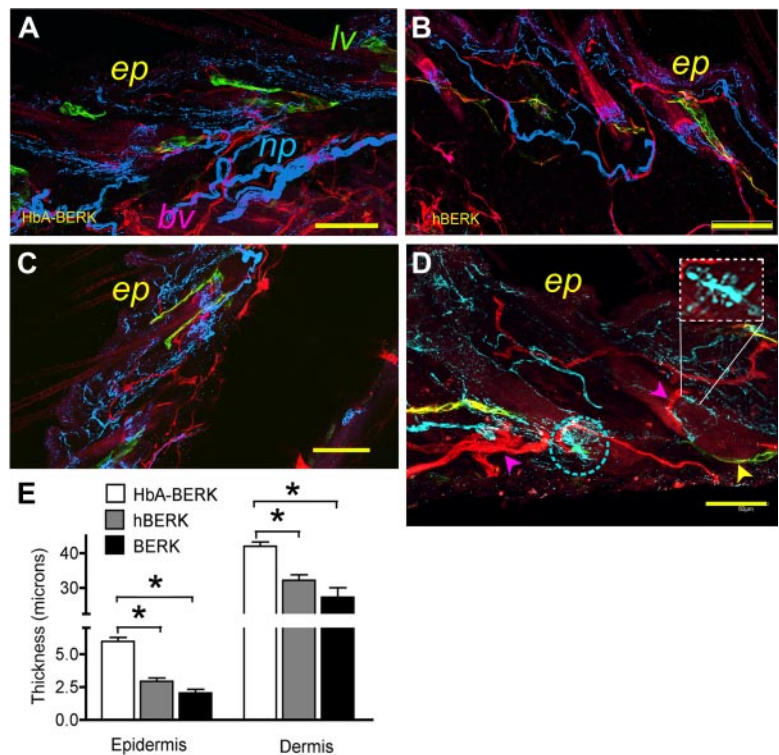


**Figure 4. Local application of CP 55940 reduces CFA-induced pain in BERK and hBERK1 mice.** PWF was assessed by the application of 1.0 g of von Frey filament in 10-month-old BERK (A) and 8-month-old male hBERK1 (B) mice and age- and sex-matched HbA-BERK mice. PWFs were recorded before and for 24 hours after injecting 10  $\mu$ g (in 10  $\mu$ L) of CFA. Then, 10  $\mu$ g (in 10  $\mu$ L) of CP 55940 or vehicle was injected in the same hind paw, and PWF recorded over another 6 hours. Data are shown as mean  $\pm$  SEM from 4 mice with 3 observations per mouse. Significance of differences: In panel A: \* $P < .05$ , after CFA versus baseline (before CFA); † $P < .01$ , immediately before versus after administration of CP 55940; ‡ $P < .01$ , CP 55940 versus vehicle at the same time point. In panel B: \* $P < .01$ , after CFA versus baseline (before CFA); † $P < .01$ , CP 55940 versus vehicle at the same time point; ‡ $P < .01$ , immediately before versus after administration of CP 55940.

**Figure 5. Laser scanning confocal microscopy and immunofluorescent microscopy of skin from male hBERK1 and matched HbA-BERK mice.** (A-D) A montage of overlapping fields of Z-stack images (each 2.5- $\mu\text{m}$ -thick) of 80- to 100- $\mu\text{m}$ -thick sections of skin in HbA-BERK (A), hBERK1 (B), and BERK (C-D), showing vascular, lymphatic, and nerve architecture. Image shows CD31<sup>+</sup> blood vessels (pseudo-colored red), PGP 9.5 immunoreactive nerves (pseudo-colored blue), and LYVE1<sup>+</sup> lymphatic vessels (pseudo-colored green). Bar represents 250  $\mu\text{m}$  (A-C) and 50  $\mu\text{m}$  (D). The rectangular inset in panel D shows an enlargement of sprouting of nerve fibers, also seen in the encircled area. *ep* indicates epidermis; *lv*, lymphatic vessels; and *np*, nerve plexus. Each image represents 3 reproducible and similar images. Image acquisition information: FluoView FV1000 Laser Scanning Confocal BX61 Microscope (Olympus); 20 $\times$ /0.70 (A-C), 40 $\times$ /1.35 (D) oil objective lenses; In-built image acquisition system; Adobe Photoshop. (E) Morphometric analysis of epidermal and dermal thickness performed on hematoxylin and eosin-stained skin sections (shown in supplemental Figure 3; original magnification  $\times$ 200) by substituting 1 unit for 0.5  $\mu\text{m}$  as per the calibration of the micrometer. Data are shown as mean  $\pm$  SEM of 9 measurements of 3 separate sections from 3 different mice.  $\square$  represents HbA-BERK mice;  $\blacksquare$ , hBERK1 mice; and  $\blacksquare$ , BERK mice. \* $P < .01$ .



which are found in nociceptive nerve fibers, was altered in the skin of BERK (Figure 6E) and hBERK1 mice (Figure 6C). We observed increased immunoreactivity for both SP and CGRP in BERK and hBERK1 skin compared with the skin of HbA-BERK mice (Figure 6A). Intense, punctate SP and CGRP immunoreactivity was seen throughout the dermis and epidermis in BERK and hBERK1 mice. In addition, localized dense clusters of SP and CGRP immunoreactivity were seen in the deep dermis in BERK skin. Enhanced expression and release of neuropeptides from terminals of nociceptive afferent fibers probably contribute to neurogenic inflammation and hyperalgesia.

MOR expression was lower in the epidermis and dermis of hBERK1 (Figure 6D) compared with HbA-BERK mice (Figure 6B). MOR expression also strongly colocalized with the CD31<sup>+</sup> blood vessels in HbA-BERK mice. The scarce blood vessels in hBERK1 mice showed relatively poor or no expression of MOR.

#### Glial activation in the spinal cord of mice expressing HbS

Because activation of spinal glia contribute to central sensitization and hyperalgesia, we examined the expression of mediators of central sensitization in the spinal cord of hBERK1 and HbA-BERK mice (Figure 7). We observed higher expression of IL-6, COX-2, and TLR4 in the spinal cord of hBERK1 compared with HbA-BERK mice (Figure 7A-B). MOR expression was lower in the spinal cord of hBERK1, as was seen in the skin of these mice. The activation of several mediators of pain, including MAPK/ERK, p38 MAPK, and STAT3 was significantly increased in the spinal cord of hBERK1 mice (Figure 7C-D). These data suggest that spinal glial and/or neuronal nociceptors are sensitized in mice expressing HbS.

## Discussion

We show that mice expressing HbS (BERK and hBERK1) exhibit spontaneous deep/musculoskeletal pain and cutaneous hyperalge-

sia to mechanical, heat, and cold stimuli. Both morphine and cannabinoid receptor agonist CP 55940 reduced hyperalgesia in mice expressing HbS. The skin of mice expressing HbS had thinner epidermal and dermal layers and decreased innervation suggestive of peripheral neuropathy. In addition, there was an increase in cutaneous expression of CGRP and SP. At the spinal cord level, there was an up-regulation of TLR4, IL-6-phospho, STAT3, COX-2, and phospho-MAPK and down-regulation of MOR. These changes may contribute to central sensitization and the accompanying hyperalgesia in mice expressing HbS.

Both BERK and hBERK1 exhibited more severe deep tissue and cutaneous hyperalgesia compared with HbA-BERK mice. The provenance of all 3 mice is identical: they were created in the same laboratory, at the same time, and on the same mixed genetic background.<sup>20</sup> Therefore, our findings are probably not simply the result of strain differences between these mice. Nevertheless, we cannot exclude the possibility that minor variation in mouse strains between BERK/hBERK1 (which are littermates) versus the control HbA-BERK may have contributed in part to observed differences in behavior. However, experiments with BERK and hBERK1 mice were also internally controlled because, within each genotype, we examined mice serially at different ages, mice of both sexes separately, and mice before and after treatment with opioids or CP 55940.

Our finding that hBERK1 mice exhibit pain-related behaviors qualitatively similar to BERK was unexpected. The reason for this is not known at present because relevant data are limited. hBERK1 mice have abnormal activation of pulmonary vein endothelium, just like BERK,<sup>18</sup> and they have renal histopathologic lesions (including inflammatory ones) that are similar to, but more severe than, hBERK2 littermates that have a higher level of HbS.<sup>21</sup> This has been interpreted as suggesting that the histopathology of hBERK1 is perhaps the result of tissue hypoxia caused by abnormally low oxygen affinity of the hybrid human  $\alpha$ /mouse  $\beta$  hemoglobin, leading to poor oxygen delivery. Ordinarily, a right-shifted oxygen dissociation curve would be expected to increase



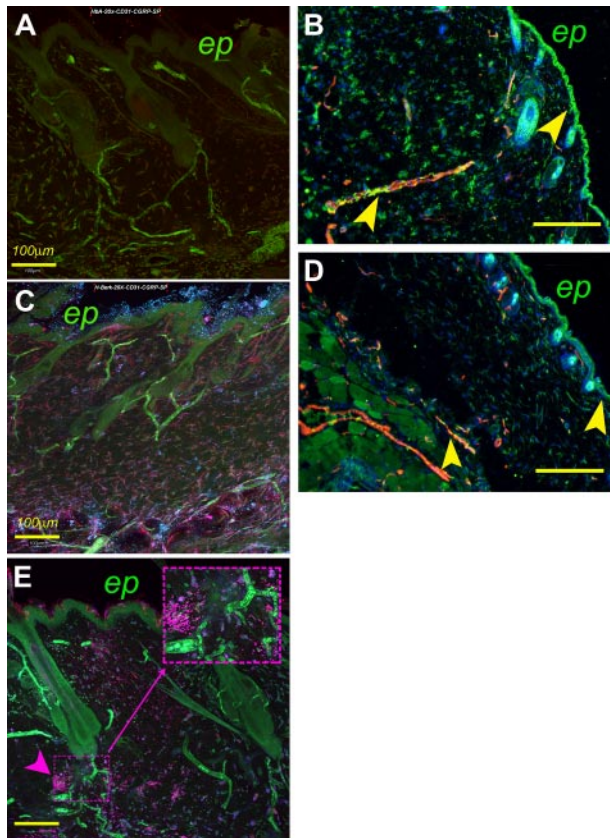


**Figure 6. A montage of overlapping fields of z-stack images (each 2.5- $\mu$ m-thick) of 80- to 100- $\mu$ m-thick sections of skin showing the expression of mediators of pain in skin.** HbA-BERK (A), hBERK1 (C), and BERK (E). Image shows CD31<sup>+</sup> blood vessels (pseudo-colored green), SP immunoreactivity (pseudo-colored red), and CGRP immunoreactivity (pseudo-colored blue). Magenta color in panels C and E is indicative of colocalization of CGRP (blue) and SP (red). The inset in panel E shows localized, dense immunoreactivity for SP in BERK mice. Bar represents 100  $\mu$ m. *ep* indicates epidermis. (B,D) Coexpression of MOR and CD31<sup>+</sup> on blood vessels in HbA-BERK (B) and hBERK1 (D) mice. Image shows CD31<sup>+</sup> blood vessels (pseudo-colored red), MOR immunoreactivity (pseudo-colored green), and 4,6-diamidino-2-phenylindole<sup>+</sup> nuclei (pseudo-colored blue). Yellow represents coexpression of MOR on blood vessels. Original magnification  $\times$ 150; scale bar represents 250  $\mu$ m. Arrows indicate MOR expression in the epidermis and vasculature. *ep* indicates epidermis. Each figure is representative of images from skins of 3 different mice. Image acquisition information: Fluoview FV1000 Laser Scanning Confocal BX61 Microscope (Olympus), 20 $\times$ /0.70 oil objective lens, In-built image acquisition system, Adobe Photoshop (panels A,C,E); Olympus IX70 microscope, 15 $\times$ /0.45 objective lens, DP70 digital camera and DP70 Manager software (Olympus), Adobe Photoshop (panels B,D).

oxygen delivery to tissues, unless it was so right-shifted as to abnormally limit oxygen loading. Consistent with that notion, Noguchi et al<sup>21</sup> observed a peculiarly increased adverse sensitivity to severe hypoxia among hBERK1 animals compared with hBERK2 littermates. Thus, it seems probable that hBERK1 mice may have deficient oxygen loading; arterial hemoglobin oxygen saturation and pO<sub>2</sub> will need to be measured to confirm this. Nonetheless, it seems conceivable that the combination of a greater degree of arterial hypoxia (from high P50) plus the effect of macromolecular crowding (also called nonideal behavior) on activity of HbS could allow some in vivo sickling of red cells in hBERK1 mice despite its relatively low ( $\sim$ 26%) level of HbS. The relatively hypoxic and acidic environment of some tissue beds (eg, renal, working muscle) would further augment this. Indeed, the latter 2 factors (even without arterial hypoxia), together with macromolecular crowding (because of high intracellular total hemoglobin concentration), allow human sickle trait red cells to sickle even though their

intracellular HbS concentration is below the acknowledged C<sub>sat</sub> required for HbS polymerization.

Thus, it is conceivable that pain characteristics observed in the hBERK1 model may be a consequence of severe inflammation, altered oxygen availability, and organ disease,<sup>18,20,21</sup> which may in turn cause perturbation in the peripheral nerves and spinal activation of pain mediators observed herein. Perhaps these behaviors are further influenced by a different degree or tissue distribution of hypoxia in hBERK1 compared with BERK mice.

### Hyperalgesia in mice expressing HbS

Increased sensitivity to cold and heat, suggestive of cutaneous hyperalgesia in mice expressing HbS, is consistent with recent observations that painful crises in patients with SCD are related, in part, to weather extremes.<sup>26,27</sup> In SCD, painful crises and musculoskeletal pain may be a consequence of skin cooling that leads to cutaneous vasoconstriction and reflex vasoconstriction in muscles.<sup>28,29</sup>

Deep hyperalgesia observed in these mice appears to recapitulate the chronic musculoskeletal pain reported by patients with SCD. Ongoing muscle soreness and joint tenderness associated with painful crises, avascular necrosis of bone, and infarction of the bone marrow occur in SCD.<sup>3,30,31</sup> These pathologic abnormalities may contribute to nociceptor activation and sensitization, leading to central sensitization and tonic hyperalgesia.

### Effects of age and sex on pain in SCD

We show that hyperalgesia in mice expressing HbS is influenced by age and sex. Older and female mice exhibited an increase in pain-associated behaviors compared with younger and male mice, respectively. Female hBERK1 (but not BERK; data not shown) uniformly showed an increase in both deep tissue and cutaneous hyperalgesia compared with male hBERK1. Similar gender- and

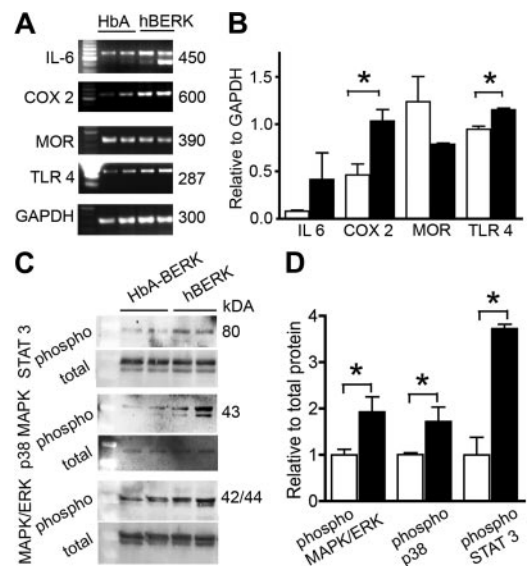


**Figure 7. Expression of inflammatory and neurochemical mediators in the spinal cords of male hBERK1 mice.** (A-B) mRNA expression using semiquantitative reverse-transcribed polymerase chain reaction. GAPDH expression shows the loading control. The first lane indicates size markers. (B) Bar represents band density for each product relative to band density of GAPDH. (C-D) Expression of phosphorylated and total proteins (MAPK/ERK, p38 MAPK, and STAT3) determined using Western immunoblotting. Bar represents band density of individual phosphoprotein relative to its total protein. (B,D) Data are the mean  $\pm$  SEM of 4 separate experiments. ■ represents hBERK1 mice; □, HbA-BERK mice. \**P* < .05.

age-based differences are observed in patients with SCD<sup>32,33</sup>: 10 to 19 years of age and females with SCD reported pain episodes of significantly longer duration, compared with less than 10 years of age and males, respectively.<sup>4</sup> Females with SCD reported higher pain intensity and number of body areas with pain compared with males, and older children reported a greater number of painful body sites than younger subjects.<sup>32</sup>

Irrespective of sex, younger mice exhibited a greater degree of deep tissue and cutaneous thermal hyperalgesia, but less tactile allodynia, even though each of these increased with age. A uniform increase in nociceptive behaviors involving forelimbs (grip force) and hind limbs (mechanical and thermal tests) with age demonstrates an increase in pain sensitivity at multiple body sites. Younger mice expressing HbS showed lower forepaw grip force (deep hyperalgesia), but no difference was observed in younger mice in PWF to von Frey filaments. Thus, as with patients with SCD, it appears that pain and hyperalgesia in mice expressing HbS increase in intensity with age. This could be a consequence of the pathologic abnormalities similar to those observed in patients with SCD.

#### Effect of morphine on hyperalgesia in mice expressing HbS

Morphine (20 mg/kg) reduced deep hyperalgesia (increased grip force) in a time-dependent fashion, whereas a lower dose (10 mg/kg) was ineffective. Doses of morphine used in mice are considerably higher than doses required for analgesia in humans because of shorter half-life of morphine in mice (“Drugs and their use”). In SCD, relatively high doses of morphine or its congeners are required to treat pain, compared with analogous pain in other diseases.<sup>4</sup> The reason for this difference in effective opioid doses is not known. It is possible that this is the result, in part, of chronic and recurrent use of opioids resulting in opioid tolerance. However, in our study, mice had not received any prior treatment with morphine, suggesting that our results were not influenced by opioid tolerance. We found a decrease in MOR expression in the skin and spinal cord of hBERK1 mice compared with controls. Decreased MOR expression was also observed in the spinal cords of mice with the Theiler murine encephalomyelitis virus-induced mouse model of multiple sclerosis.<sup>22</sup> Reduction in MOR expression in the spinal cord correlated with the development of thermal and mechanical hyperalgesia in hBERK1. MOR is expressed on nerve terminals, neurons, axons, and afferent fibers, and thereby facilitates analgesia.<sup>34</sup> The requirement of higher doses of morphine to treat pain in SCD may be related to decreased MOR expression in the spinal cord and periphery. In addition, increased clearance and metabolism of morphine in SCD may contribute to the increased requirement of morphine.<sup>4,6</sup>

#### Cannabinoid receptor agonist ameliorates hyperalgesia in mice expressing HbS

Because chronic opioid administration frequently causes troublesome side effects, we also investigated whether cannabinoids might be effective in treating pain in SCD. Clinically available cannabinoids, such as Sativex ( $\Delta^9$ -tetrahydrocannabinol + cannabidiol), an oromucosal spray, and oral Dronabinol ( $\Delta^9$ -tetrahydrocannabinol), a CB1 and CB2 cannabinoid receptor agonist, are effective in treating chronic pain in multiple sclerosis and central pain states, and pain that persisted on opioids in cancer, fibromyalgia, and rheumatoid arthritis.<sup>12,13</sup> We expect that, because of their manageable side effects and opioid-sparing activity,<sup>12</sup> newer cannabinoids may be received more favorably than crude cannabis-derived preparations by the medical, legislative, and judicial communities.

We used a synthetic CB1 and CB2 receptor agonist, CP 55940, which mimics the effect of tetrahydrocannabinol found in marijuana. It is effective in low doses to treat acute and chronic pain in animal models.<sup>35</sup> Indeed, we found that systemic administration of CP 55940 attenuated deep tissue hyperalgesia in mice expressing HbS. In a retrospective survey of 86 patients with SCD evaluating symptom relief, cannabis (marijuana) smoking reduced pain in 52% patients, led to a decrease in doses of other analgesics, and relieved anxiety and depression.<sup>36</sup> Our studies are consistent with this clinical study and underscore the need for prospective clinical trials to determine the efficacy of cannabinoids to treat pain in SCD.

Intraplantar injection of CP 55940 also attenuated hyperalgesia produced by CFA-induced inflammation in mice expressing HbS. This antihyperalgesic effect was the result of peripheral mechanisms because no catalepsy was observed. In other conditions, activation of cannabinoid receptors in the periphery reduces hyperalgesia after inflammation.<sup>37,38</sup> Importantly, we also observed strong expression of CB1 and CB2 receptors in the brain and spinal cord, and to a similar extent in younger and older hBERK1 and BERK mice (data not shown). This could contribute to the effectiveness of a relatively low dose of CP 55940, whereas a relatively higher dose of morphine is required because of the lower expression of MOR. Collectively, our data suggest that cannabinoids may be effective in treating both chronic as well as acute, localized pain associated with SCD.

Because SCD induces an inflammatory state,<sup>39</sup> it is probable that pain in this disease is at least partly neuroinflammatory in nature. Consistent with this notion, we observed an increase in systemic as well as spinal expression of the inflammatory cytokine IL-6 in mice expressing HbS compared with controls. Similar to observations by others,<sup>39,40</sup> serum levels of several cytokines were higher in hBERK1 mice compared with HbA-BERK mice: IL-1 $\alpha$  (1.5-fold), IL-6 (3-fold), chemokine (C-C motif) ligand 5 (14-fold), and tumor necrosis factor  $\alpha$  (2-fold; data not shown), indicative of a systemic inflammatory state.

#### Structural and neurochemical changes in mice expressing HbS

Mice expressing HbS exhibited a variety of structural and neurochemical changes in the periphery and spinal cord. BERK and hBERK1 skin was less innervated, and the epidermis and dermis were thinner than in control HbA-BERK. The epidermis of MOR knockout mice is thinner than that of wild-type mice.<sup>41</sup> Selective loss of motor and sensory nerve after neuronal injury also results in epidermal thinning.<sup>42</sup> Therefore, down-regulation of MOR and reduction in innervation of the skin of mice expressing HbS, as observed by us, may contribute to thinning of the epidermis. A decrease in innervation is also indicative of peripheral neuropathy and suggests a neuropathic pain condition. Sprouting and perhaps regeneration of nerve fibers seen near the areas of nerve loss in BERK skin appear to be similar to those shown in neuropathic and inflammatory pain models.<sup>43</sup> Because lymphatic vessels are involved in immune cell trafficking, stringy and distorted lymphatic vessels in hBERK1 and BERK may be dysfunctional and therefore contribute to inflammation. Further, increased expression of CGRP and SP in the skin is suggestive of neurogenic inflammation. Dilated vessels in BERK may be the result of increased CGRP, a known vasodilator. CGRP and SP are increased in persistent and inflammatory pain states.<sup>22,44</sup> Increased release of CGRP and SP may contribute to sensitization of nociceptors and hyperalgesia.<sup>16</sup> It appears that the inflammatory state in hBERK1 and BERK may be



further compounded by proinflammatory pain mediators and neurogenic inflammation.

The transgenic mice used in the present study may be useful in identifying neural mechanisms of pain in SCD. These mice exhibit musculoskeletal and cutaneous hyperalgesia, and structural and neurochemical changes in the periphery and in the spinal cord that may contribute to sensitization of nociceptors and dorsal horn neurons. Our observations in these mice suggest that both systemically administered and locally applied cannabinoids may be beneficial in treating pain in SCD.

## Acknowledgments

The authors thank Dr Cheryl Hillery for providing some BERK mice used in this study; Jonathan Henriksen, Tou Sue Vang, Niroop S. Ambashankar, and Catherine Harding-Rose for technical assistance; Carol Taubert for assistance with manuscript preparation; and Dr George L. Wilcox (University of Minnesota) for discussions and suggestions regarding this manuscript.

This work was supported by the National Institutes of Health (grants HL068802, K.G.; HL55552, R.P.H.; and DA011471, D.A.S.) and the Veterans Health Administration (P.G.).

## References

- Ballas SK. *Progress in Pain Research and Management*, vol 11. Seattle, WA: IASP Press; 1998.
- Smith WR, Penberthy LT, Bovbjerg VE, et al. Daily assessment of pain in adults with sickle cell disease. *Ann Intern Med*. 2008;148(2):94-101.
- Ballas SK. Current issues in sickle cell pain and its management. *Hematology Am Soc Hematol Educ Program*. 2007:97-105.
- Dampier CD, Setty BN, Logan J, Ioli JG, Dean R. Intravenous morphine pharmacokinetics in pediatric patients with sickle cell disease. *J Pediatr*. 1995;126(3):461-467.
- Darbari DS, Minniti CP, Rana S, van den Anker J. Pharmacogenetics of morphine: potential implications in sickle cell disease. *Am J Hematol*. 2008;83(3):233-236.
- Nagar S, Rimmel RP, Hebbel RP, Zimmerman CL. Metabolism of opioids is altered in liver microsomes of sickle cell transgenic mice. *Drug Metab Dispos*. 2004;32(1):98-104.
- Kopecky EA, Jacobson S, Joshi P, Koren G. Systemic exposure to morphine and the risk of acute chest syndrome in sickle cell disease. *Clin Pharmacol Ther*. 2004;75(3):140-146.
- Weber ML, Farooqui M, Nguyen J, et al. Morphine induces mesangial cell proliferation and glomerulopathy via kappa-opioid receptors. *Am J Physiol Renal Physiol*. 2008;294(6):F1388-F1397.
- Khasabova IA, Khasabov SG, Harding-Rose C, et al. A decrease in anandamide signaling contributes to the maintenance of cutaneous mechanical hyperalgesia in a model of bone cancer pain. *J Neurosci*. 2008;28(44):11141-11152.
- Cheng Y, Hitchcock SA. Targeting cannabinoid agonists for inflammatory and neuropathic pain. *Expert Opin Investig Drugs*. 2007;16(7):951-965.
- Anand P, Whiteside G, Fowler CJ, Hohmann AG. Targeting CB2 receptors and the endocannabinoid system for the treatment of pain. *Brain Res Rev*. 2009;60(1):255-266.
- Elikkottil J, Gupta P, Gupta K. The analgesic potential of cannabinoids. *J Opioid Manag*. 2009;5(6):341-357.
- Johnson JR, Burnell-Nugent M, Lossignol D, Ganae-Motan ED, Potts R, Fallon MT. Multi-center, double-blind, randomized, placebo-controlled, parallel-group study of the efficacy, safety, and tolerability of THC:CBD extract and THC extract in patients with intractable cancer-related pain. *J Pain Symptom Manage*. 2010;39(2):167-179.
- Rog DJ, Nurmiikko TJ, Young CA. Oromucosal delta9-tetrahydrocannabinol/cannabidiol for neuropathic pain associated with multiple sclerosis: an uncontrolled, open-label, 2-year extension trial. *Clin Ther*. 2007;29(9):2068-2079.
- Watkins LR, Hutchinson MR, Milligan ED, Maier SF. "Listening" and "talking" to neurons: implications of immune activation for pain control and increasing the efficacy of opioids. *Brain Res Rev*. 2007;56(1):148-169.
- Li D, Ren Y, Xu X, Zou X, Fang L, Lin Q. Sensitization of primary afferent nociceptors induced by intradermal capsaicin involves the peripheral release of calcitonin gene-related peptide driven by dorsal root reflexes. *J Pain*. 2008;9(12):1155-1168.
- Manci EA, Hillery CA, Bodian CA, Zhang ZG, Luty GA, Collier BS. Pathology of Berkeley sickle cell mice: similarities and differences with human sickle cell disease. *Blood*. 2006;107(4):1651-1658.
- Solovey A, Kollander R, Shet A, et al. Endothelial cell expression of tissue factor in sickle mice is augmented by hypoxia/reoxygenation and inhibited by lovastatin. *Blood*. 2004;104(3):840-846.
- Lunzer MM, Yekkirala A, Hebbel RP, Portoghesi PS. Naloxone acts as a potent analgesic in transgenic mouse models of sickle cell anemia. *Proc Natl Acad Sci U S A*. 2007;104(14):6061-6065.
- Pászty C, Brion CM, Manci E, et al. Transgenic knockout mice with exclusively human sickle hemoglobin and sickle cell disease. *Science*. 1997;278(5339):876-878.
- Noguchi CT, Gladwin M, Diwan B, et al. Pathophysiology of a sickle cell trait mouse model: human alpha(beta)(S) transgenes with one mouse beta-globin allele. *Blood Cells Mol Dis*. 2001;27(6):971-977.
- Lynch JL, Gallus NJ, Ericson ME, Beitz AJ. Analysis of nociception, sex and peripheral nerve innervation in the TMEM animal model of multiple sclerosis. *Pain*. 2008;136(3):293-304.
- Tapocik JD, Letwin N, Mayo CL, et al. Identification of candidate genes and gene networks specifically associated with analgesic tolerance to morphine. *J Neurosci*. 2009;29(16):5295-5307.
- Ishikawa K, McGaugh JL, Shibasaki S, Kubo T. A sensitive procedure for determination of morphine in mouse whole blood by high performance liquid chromatography with electrochemical detection. *Jpn J Pharmacol*. 1982;32(5):969-971.
- Poonawala T, Levay-Young BK, Hebbel RP, Gupta K. Opioids heal ischemic wounds in the rat. *Wound Repair Regen*. 2005;13(2):165-174.
- Smith WR, Bauserman RL, Ballas SK, et al. Climatic and geographic temporal patterns of pain in the Multicenter Study of Hydroxyurea. *Pain*. 2009;146(1):91-98.
- Westerman MP, Bailey K, Freels S, Schlegel R, Williamson P. Assessment of painful episode frequency in sickle-cell disease. *Am J Hematol*. 1997;54(3):183-188.
- Serjeant GR, Chalmers RM. Current concerns in haematology: 1. Is the painful crisis of sickle cell disease a "steal" syndrome? *J Clin Pathol*. 1990;43(10):789-791.
- Mohan J, Marshall JM. A comparative study in subjects with homozygous sickle cell disease and in normal subjects of responses evoked in forearm vasculature by mild, indirect cooling. *Clin Auton Res*. 1994;4(1):35-40.
- Ejindu VC, Hine AL, Mashayekhi M, Shorvon PJ, Misra RR. Musculoskeletal manifestations of sickle cell disease. *Radiographics*. 2007;27(4):1005-1021.
- Jain R, Sawhney S, Rizvi SG. Acute bone crises in sickle cell disease: the T1 fat-saturated sequence in differentiation of acute bone infarcts from acute osteomyelitis. *Clin Radiol*. 2008;63(1):59-70.
- Franck LS, Treadwell M, Jacob E, Vichinsky E. Assessment of sickle cell pain in children and young adults using the adolescent pediatric pain tool. *J Pain Symptom Manage*. 2002;23(2):114-120.
- Sporrer KA, Jackson SM, Agner S, Laver J, Abboud MR. Pain in children and adolescents with sickle cell anemia: a prospective study utilizing self-reporting. *Am J Pediatr Hematol Oncol*. 1994;16(3):219-224.

34. Ballet S, Conrath M, Fischer J, Kaneko T, Hamon M, Cesselin F. Expression and G-protein coupling of mu-opioid receptors in the spinal cord and dorsal root ganglia of polyarthritic rats. *Neuropeptides*. 2003;37(4):211-219.
35. Hamamoto DT, Giridharagopalan S, Simone DA. Acute and chronic administration of the cannabinoid receptor agonist CP 55940 attenuates tumor-evoked hyperalgesia. *Eur J Pharmacol*. 2007;558(1):73-87.
36. Howard J, Anie KA, Holdcroft A, Korn S, Davies SC. Cannabis use in sickle cell disease: a questionnaire study. *Br J Haematol*. 2005;131(1):123-128.
37. Potenziari C, Brink TS, Pacharinsak C, Simone DA. Cannabinoid modulation of cutaneous Adelta nociceptors during inflammation. *J Neurophysiol*. 2008;100(5):2794-2806.
38. Guindon J, Hohmann AG. Cannabinoid CB2 receptors: a therapeutic target for the treatment of inflammatory and neuropathic pain. *Br J Pharmacol*. 2008;153(2):319-334.
39. Hebbel RP, Osarogiagbon R, Kaul D. The endothelial biology of sickle cell disease: inflammation and a chronic vasculopathy. *Microcirculation*. 2004;11(2):129-151.
40. Belcher JD, Bryant CJ, Nguyen J, et al. Transgenic sickle mice have vascular inflammation. *Blood*. 2003;101(10):3953-3959.
41. Bigliardi-Qi M, Gaveriaux-Ruff C, Pfaltz K, et al. Deletion of mu- and kappa-opioid receptors in mice changes epidermal hypertrophy, density of peripheral nerve endings, and itch behavior. *J Invest Dermatol*. 2007;127(6):1479-1488.
42. Li Y, Hsieh ST, Chien HF, Zhang X, McArthur JC, Griffin JW. Sensory and motor denervation influence epidermal thickness in rat foot glabrous skin. *Exp Neurol*. 1997;147(2):452-462.
43. Almarestani L, Longo G, Ribeiro-da-Silva A. Autonomic fiber sprouting in the skin in chronic inflammation. *Mol Pain*. 2008;4:56.
44. Honore P, Rogers SD, Schwei MJ, et al. Murine models of inflammatory, neuropathic and cancer pain each generates a unique set of neurochemical changes in the spinal cord and sensory neurons. *Neuroscience*. 2000;98(3):585-598.